Research Square

Preprints are preliminary reports that have not undergone peer review.
They should not be considered conclusive, used to inform clinical practice,
or referenced by the media as validated information.

Mucosal mRNA-sLNP boosting following BCG vaccination induces local pulmonary immunity with limited inflammation

Ana Maria Valencia-Hernandez
James Cook University
Guangzu Zhao
James Cook University
Julia Seifert
James Cook University
Harindra D. Sathkumara
James Cook University
Socorro Miranda-Hernadez
James Cook University
Munish Puri
James Cook University
Andreas Kupz
andreas.kupz@jcu.edu.au
James Cook University

Article

Keywords: Tuberculosis, vaccine development, mRNA vaccine, mucosal vaccination, BCG, prime-and-pull.

Posted Date: November 11th, 2026

DOI: https://doi.org/10.21203/rs.3.rs-11370478/v1

License: This work is licensed under a Creative Commons Attribution 4.0 International License.
Read Full License

Additional Declarations: No competing interests reported.

Mucosal mRNA-sLNP boosting following BCG vaccination induces local pulmonary immunity with limited inflammation

Ana Maria Valencia-Hernandez[1], Guangzu Zhao[1], Julia Seifert[1], Harindra D. Sathkumara[1], Socorro Miranda-Hernadez[1], Munish Puri[1], Andreas Kupz[1*].

[1]Australian Institute of Tropical Health and Medicine, James Cook University, Cairns & Townsville, QLD, Australia.

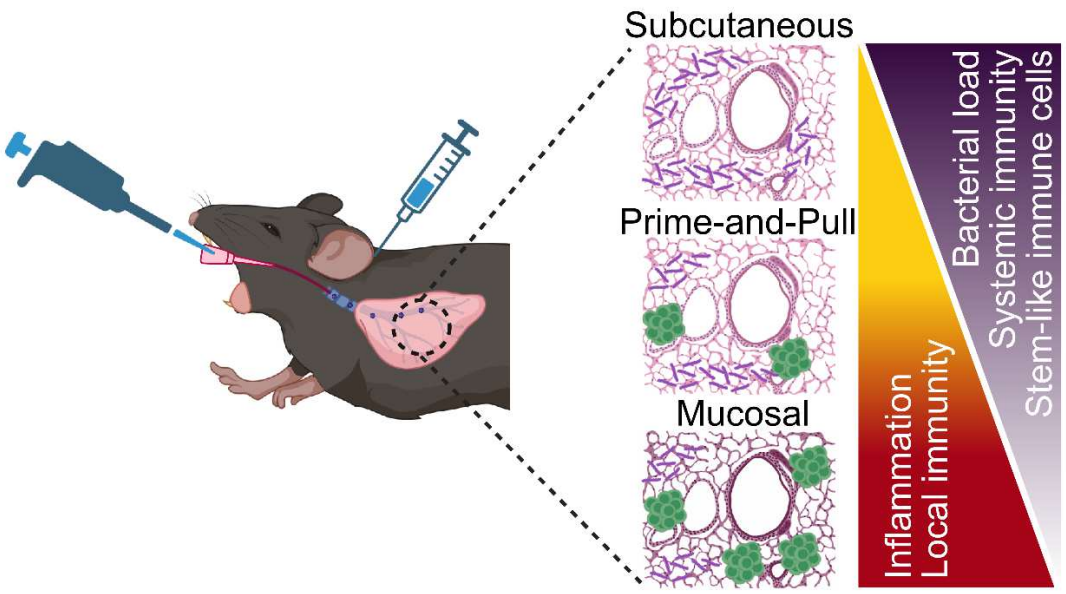
*Correspondence should be addressed to A.K. (andreas.kupz@jcu.edu.au)

Abstract

Pulmonary vaccination improves protection against tuberculosis by generating immune responses at the primary site of *Mycobacterium tuberculosis* infection. However, pulmonary delivery of live vaccines can induce excessive inflammation and raises safety concerns. Here, we developed an mRNA-based prime-and-pull strategy in which subcutaneous BCG vaccination was followed by pulmonary delivery of mRNA formulated in stealth lipid nanoparticles. Pulmonary mRNA delivery supported protein expression in multiple lung cell populations. Using ESAT-6 as a model antigen, pulmonary mRNA boosting enhanced antigen-specific and memory T cell responses beyond those induced by mRNA alone. A multivalent mRNA formulation encoding eight selected *M. tuberculosis*- and BCG-derived antigens induced pulmonary T cell responses comparable to subcutaneous BCG vaccination, increased antibody reactivity, and increased stem cell-like memory T cell frequencies. Prime-and-pull vaccination reduced pulmonary inflammation and pathology relative to pulmonary BCG vaccination while maintaining protection comparable to subcutaneous BCG.

Keywords

Tuberculosis, vaccine development, mRNA vaccine, mucosal vaccination, BCG, prime-and-pull.



Graphical Abstract

Introduction

The only licensed tuberculosis (TB) vaccine, *Mycobacterium bovis* Bacillus Calmette-Guérin (BCG), protects children against severe forms of disease, reduces all-cause infant mortality, and confers heterologous protection against multiple infectious diseases beyond childhood.[1-5] However, protection against pulmonary TB (the most prevalent and transmissible form of the disease) varies widely, ranging from >70% in Nordic countries to <20% in TB-endemic regions.[6-11] As a result, there is an urgent need for more effective TB vaccination strategies, particularly in settings where BCG efficacy is lowest. Although several vaccine candidates have advanced through clinical development over recent decades, none have surpassed BCG in protective efficacy, which remains the benchmark for TB vaccination.[12]

Mucosal vaccination has emerged as an attractive approach because it can local enhance immune responses, induce tissue resident memory T cells (T_{RM}) at the site of pathogen entry and, in some experimental models, has provided greater protection than conventional parenteral delivery.[13-15] Effective mucosal immunization requires a finely tuned inflammatory response that promotes immunity while preserving tissue integrity and function.

To date, only a limited number of mucosal-delivered TB vaccine candidates have entered clinical evaluation. These include viral-vectored vaccines expressing *Mycobacterium tuberculosis* (*Mtb*) antigens, such as MVA85A, AdHu5Ag85A, ChAdOx1-85A, and TB/FLU-05E, which have been assessed for safety following aerosol or intranasal administration in Phase I trials.[16-20] Among live-attenuated vaccines (LAVs), recent studies have investigated aerosolized BCG as a controlled

challenge model in vaccinated and unvaccinated individuals (NCT02709278, NCT06670755, NCT06246851, NCT03912207, NCT04777721).[21] High-dose aerosol BCG was generally well tolerated, with only a trend toward increased adverse events.[21] Nevertheless, concerns remain regarding potentially uncontrolled replication and excessive inflammation following mucosal delivery of LAVs, underscoring the need for alternative strategies.

To address these challenges, we sought to develop an mRNA-based prime-and-pull vaccination strategy designed to preserve immunogenicity while limiting inflammation and avoiding the risk of microbial replication. We hypothesised that subcutaneous BCG priming would establish systemic immunity, followed by pulmonary administration of a lipid nanoparticle (LNP)-formulated multivalent mRNA vaccine to provide transient local antigenic stimulation within the lung. Because T_{RM} cells contribute to protection against pulmonary TB, we further hypothesised that pulmonary mRNA boosting would promote the recruitment and accumulation of antigen-specific T cell populations expressing tissue-residency markers at site of infection. Because conventional mRNA vaccines are non-replicating, we further hypothesised that this approach would reduce the inflammatory burden associated with pulmonary administration of live mycobacteria.

We first evaluated whether customized LNPs could deliver mRNA to lung cells and support local protein expression in vivo. Using the well-characterized, immunodominant *Mtb*-derived 6 kDa early secretory antigenic target (ESAT-6) as a model antigen, we then showed that a single high-dose prime-and-pull regimen, rather than multiple low-dose administrations, induced robust populations of polyfunctional

antigen-specific T cells in the lungs of vaccinated mice, with minimal cellular infiltration relative to mucosal BCG vaccination. Guided by these findings, we next selected eight *Mtb*- and BCG-derived antigens to generate four multi-antigen mRNA constructs formulated in customized LNPs as a proof-of-principle evaluation of a broader multivalent strategy. *In vivo* vaccination and challenge studies showed that this prime-and-pull approach was well tolerated in mice and supported protective immunity in a murine model. Collectively, these findings provide proof of concept for a modular mRNA-based prime-and-pull strategy that can enhance local pulmonary immunity while limiting the inflammatory pathology associated with pulmonary BCG vaccination.

Results

Pulmonary delivery of GFP-mRNA using sLNPs

Effective delivery of mRNA to the respiratory tract requires overcoming physiological barriers including mucus, mucociliary clearance, and uptake by phagocytic cells. To address these challenges, customized stealth lipid nanoparticles (sLNPs) were used for intratracheal (IT) delivery of mRNA. sLNPs incorporate polyethylene glycol (PEG)-containing lipids that improve colloidal stability, reduce nonspecific interactions, and protect nucleic acid cargo from degradation. Previous studies have demonstrated efficient pulmonary delivery of nucleic acids using related formulations.[22-24]

To evaluate whether sLNPs could support mRNA delivery and protein expression in the lung, commercially available eGFP mRNA was formulated into sLNPs and administered via the IT route (Fig. 1A). GFP expression was assessed by flow cytometry 24 h and 48 h after administration. Representative gating strategies and

GFP expression plots for the analysed pulmonary cell populations are shown in Supplementary Fig. 1. GFP-positive cells were detected in multiple lung cell populations following IT administration of GFP-mRNA-sLNPs (Fig. 1B-D), in particular neutrophils demonstrated detectable GFP expression at both time points relative to PBS control animals (Fig. 1B). Quantification of GFP-positive cells revealed expression in multiple pulmonary cell populations, including interstitial macrophages (IMs), dendritic cells (DCs), and neutrophils (Fig. 1C). GFP-positive cell numbers increased between 24 h and 48 h post-administration, with the highest numbers observed among DCs and neutrophils at 48 h, whereas IMs showed a similar trend that did not reach statistical significance.

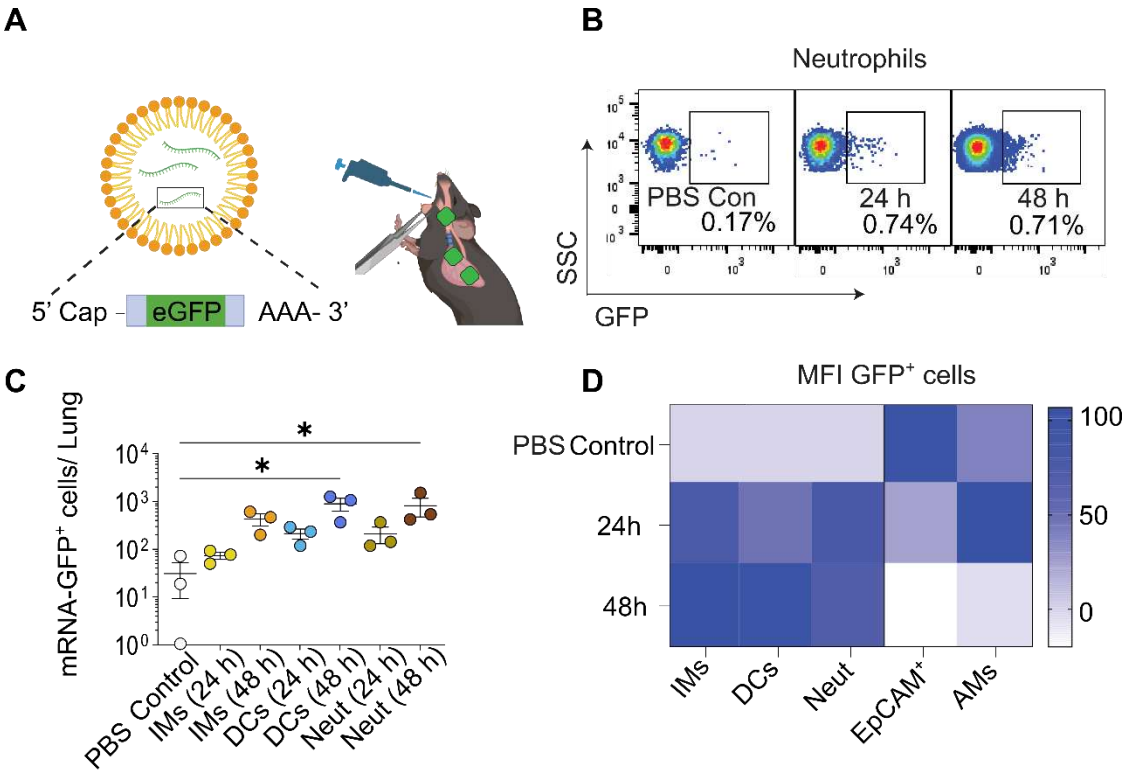


Figure 1. GFP expression by lung cells following intratracheal administration of GFP-mRNA-sLNPs. **A.** Schematic representation of GFP-mRNA formulation in stealth lipid nanoparticles (sLNPs) and intratracheal (IT) administration. Mice received either PBS (control) or 10 µg GFP-mRNA-sLNPs. Lungs were harvested 24 h and 48 h following administration. GFP expression was assessed in individual pulmonary cell populations by flow cytometry. **B.** Representative concatenated flow cytometry plots showing GFP expression in neutrophils. **C.** Number of GFP⁺ interstitial macrophages (IMs), dendritic cells (DCs), and neutrophils in the lungs. **D.** Heat map showing the mean fluorescence intensity (MFI) of GFP-positive cells, including IMs, DCs, neutrophils, EpCAM⁺ epithelial cells, and alveolar macrophages (AMs). Representative gating strategies and GFP expression plots for pulmonary cell populations are shown in Supplementary Fig. 1. Data were analysed using ordinary one-way

ANOVA with Dunnett's multiple-comparison test, with each group compared to the PBS control. Symbols represent individual animals and bars indicate the mean ± SEM. $P < 0.05$.

Analysis of GFP fluorescence intensity further demonstrated successful transgene expression following mRNA delivery (Fig. 1D). GFP signal was detected in all analysed cell populations, with the highest fluorescence intensity observed in DCs. GFP fluorescence was also detected in $EpCAM^+$ epithelial cells and alveolar macrophages (AMs); however, interpretation of these populations was limited by intrinsic autofluorescence within the GFP detection channel.

Together, these data show that intratracheally administered GFP-mRNA-sLNPs deliver functional mRNA to multiple pulmonary cell populations and support local protein expression for at least 48 h following administration.

Pulmonary delivery of ESAT-6-mRNA enhances antigen-specific T cell responses in BCG-primed mice

We next performed proof-of-concept studies using the immunodominant *Mtb*-derived Early Secreted Antigenic Target 6 (ESAT-6) as a model antigen to characterize antigen-specific immune responses induced by the prime-and-pull vaccination strategy. Customized ESAT-6 mRNA was formulated in sLNPs using the same conditions as for GFP experiments. Mice were primed with recombinant BCG expressing ESAT-6 (BCG::RD1), administered either SC or IT (Fig. 2A). Following SC BCG::RD1 priming, prime-and-pull mice received IT ESAT-6-mRNA-sLNPs according to one of four boosting regimens: P&P-E6 (5 µg × 1), P&P-E6 (5 µg × 2), P&P-E6 (5 µg × 3), or P&P-E6 (10 µg × 1), corresponding to one, two, or three 5 µg doses, or a single 10 µg dose, respectively (Fig. 2B). Antigen-specific T-cell responses were

analysed 28 days following primary vaccination, corresponding to the reported peak of pulmonary T-cell accumulation following intratracheal BCG vaccination.[25]

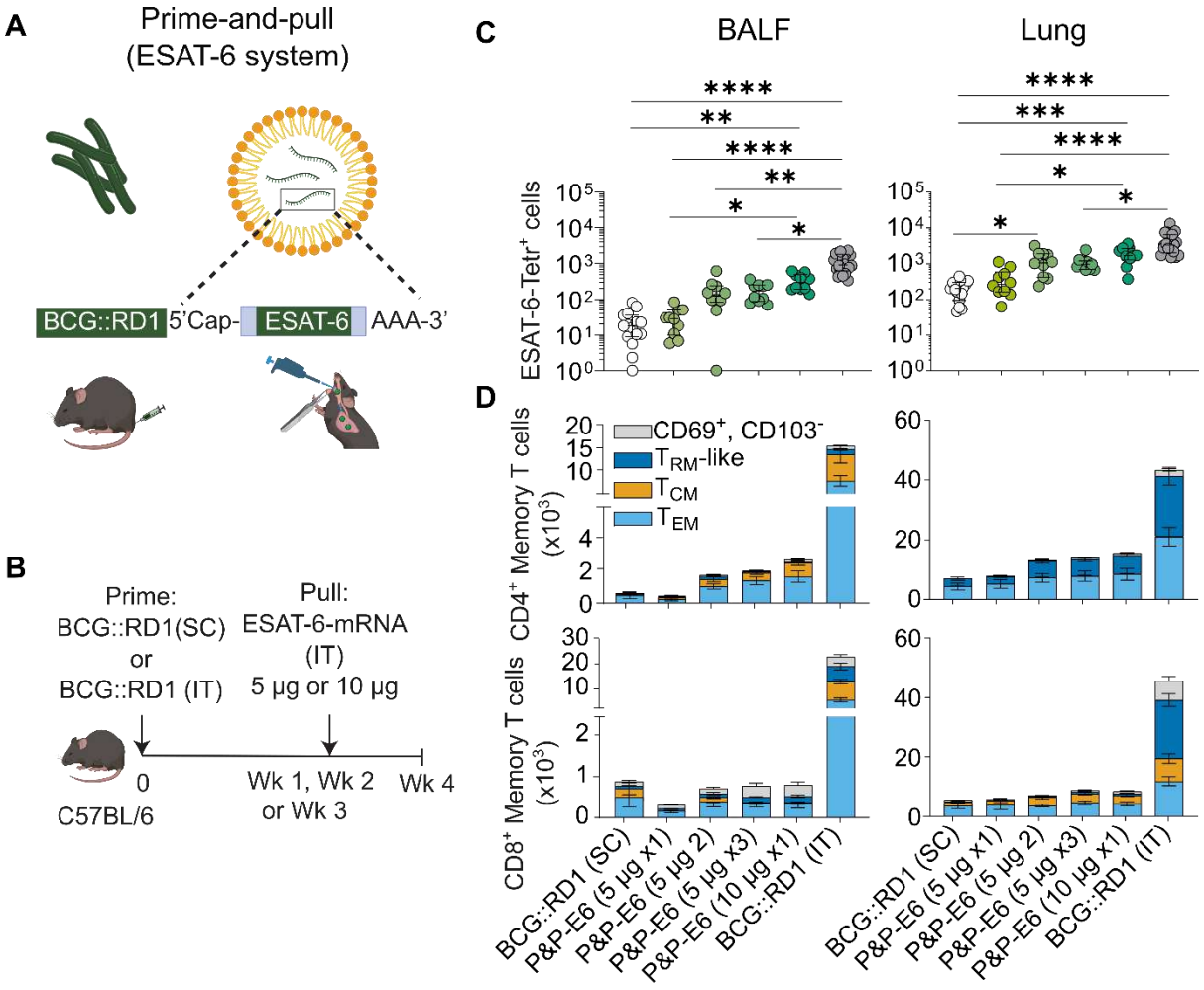


Figure 2. Pulmonary ESAT-6 mRNA boosting induces antigen-specific and memory T cell responses following BCG priming. A. Schematic representation of the prime-and-pull vaccination strategy using BCG::RD1 priming followed by pulmonary administration of ESAT-6-mRNA-sLNPs. **B.** C57BL/6 mice were vaccinated with BCG::RD1 either subcutaneously (SC; 1 × 10^6 CFU) or intratracheally (IT; 1 × 10^5 CFU). Following SC BCG::RD1 priming, mice received pulmonary ESAT-6-mRNA-sLNP boosting according to one of four regimens: P&P-E6 (5 µg × 1), P&P-E6 (5 µg × 2), P&P-E6 (5 µg × 3), or P&P-E6 (10 µg × 1). Antigen-specific and memory T-cell responses were analysed 28 days following primary vaccination. **C.** Number of ESAT-6 tetramer$^+$ cells in bronchoalveolar lavage fluid (BALF) and lungs. **D.** Number of CD4$^+$ and CD8$^+$ memory T cell populations, including CD69$^+$CD103$^-$ cells, T_{RM}-like cells, T_{CM} cells, and T_{EM} cells, in BALF and lungs. Data were analysed using the Kruskal-Wallis test with Dunn's multiple-comparison post-test. NE = 2-3 independent experiments; *n* = 4-5 mice per group. Symbols represent individual animals and bars indicate the median and interquartile range (IQR). **P*<0.05, ***P*<0.01, ****P*<0.001, *****P*< 0.0001.

A single pulmonary administration of 10 µg ESAT-6 mRNA induced significantly greater numbers of ESAT-6 tetramer$^+$ T cells in both bronchoalveolar lavage fluid (BALF) and lung tissue compared with SC BCG::RD1 vaccination alone (Fig. 2C).

Repeated administration of lower mRNA doses (5 µg) produced a progressive increase in tetramer$^+$ T cell numbers, although the single 10 µg dose consistently generated the strongest response among the mRNA-boosted groups. Importantly, prime-and-pull vaccination induced higher numbers of ESAT-6-specific T cells than either SC BCG::RD1 vaccination alone or pulmonary administration of ESAT-6 mRNA without prior BCG priming (Supp. Fig. 2A-D), supporting the contribution of both systemic priming and local pulmonary boosting to the observed response. IT BCG::RD1 vaccination induced the highest overall numbers of antigen-specific T cells; however, these responses were not significantly greater than those generated by the 10 µg prime-and-pull regimen (Fig. 2C).

Analysis of memory T-cell populations revealed a similar pattern. A single 10 µg IT ESAT-6 mRNA boost significantly increased CD4$^+$ memory T cell numbers in BALF and lungs compared with SC BCG::RD1 vaccination alone (Fig. 2D). In contrast, a single 5 µg administration produced little change relative to SC BCG::RD1 vaccination. The number of antigen-specific and memory T cells increased progressively with repeated low-dose mRNA administration, suggesting a dose-dependent effect of pulmonary mRNA boosting. IT BCG::RD1 vaccination induced the greatest accumulation of pulmonary memory T cells, particularly T_{EM} and T_{RM}-like populations, whereas the prime-and-pull regimen generated intermediate responses that exceeded those induced by SC vaccination alone.

Consistent with systemic priming by SC BCG::RD1 vaccination, no major differences in antigen-specific or memory T cell populations were observed in the spleen across vaccination groups (Supp. Fig. 3A, C and D). IT BCG::RD1 vaccination also induced

elevated numbers of ESAT-6-specific T cells in the spleen, suggesting broader dissemination of antigen-specific responses following pulmonary vaccination. In the mediastinal lymph nodes (medLN), IT BCG::RD1 induced the highest numbers of antigen-specific T cells, while the single 10 µg prime-and-pull regimen showed a trend toward increased responses compared with SC BCG::RD1 alone (Supp. Fig. 3B).

Given the transient nature of pulmonary T cell accumulation, we next assessed responses at day 56 following vaccination, focusing on SC BCG::RD1, single-dose prime-and-pull, and IT BCG::RD1 groups. Both IT BCG::RD1 vaccination and prime-and-pull vaccination induced transient increases in antigen-specific and memory T cell populations in BALF, lung, medLN, and spleen (Supp. Fig. 3E-H). The most pronounced decline between days 28 and 56 was observed in lungs of IT BCG::RD1-vaccinated mice.

Together, these findings demonstrate that pulmonary ESAT-6 mRNA boosting enhances local antigen-specific and memory T cell responses following SC BCG::RD1 priming. The greater accumulation of ESAT-6-specific T cells following prime-and-pull vaccination compared with either SC BCG::RD1 or mRNA vaccination alone is consistent with a prime-and-pull effect, with a single 10 µg mRNA dose producing the strongest responses.

Immunogenicity of a multivalent mRNA prime-and-pull vaccination strategy

Although BCG::RD1 provides enhanced protection in experimental TB models compared with conventional BCG, safety concerns associated with pulmonary administration of live recombinant mycobacteria may limit its suitability for human

227 vaccination. [26,27] We therefore evaluated a prime-and-pull strategy using conventional
228 BCG priming combined with pulmonary delivery of a multivalent mRNA formulation
229 encoding eight selected *Mtb*- and BCG-derived antigens. Proteins were selected
230 based on immune recognition in humans and mice, inclusion of T and B cell epitopes,
231 expression during infection, and previous incorporation into TB vaccine candidates
232 (Table 1).

233 **Table1.** Selection of antigens and their immunological characteristics.

Antigen	Function and location	Vaccine candidate	Expression
HBHA (Heparin-binding hemagglutinin adhesin)	Exposed-surface protein involved in adherence to epithelial cells. [28]	Pre-clinical data available.[29]	*Mtb* / BCG
HRP1 (Hypoxic response protein 1, Rv2626c)	Protein present in the cytoplasm, membrane and cell-wall with linked to latency phase of the disease.[30]	MVATG18598 (pre-clinical).[31,32]	*Mtb* / BCG
HspX (Rv2031c)	Chaperone protein associated with latency and present in the cytoplasm, membrane and cell wall.[33]	TB/FLU-05E (phase II clinical trials).	*Mtb* / BCG
CFP10 (Rv3874, esxB)	Secreted protein involved in bacterial escape and immune modulation.[33]	AEC/BC02 (phase II), MVATG18598 (pre-clinical), GamTBvac (phase III).	*Mtb*
Ag85b (Rv1886c)	Cell wall biogenesis and immune response. Secreted protein.[33]	AEC/BC02 (phase II), H56:IC31 (phase IIb), MVATG18598 (pre-clinical), ID91 repRNA (pre-clinical).	*Mtb* / BCG

VapB47 (Rv3407)	Antitoxin for VapC47 toxin. Binds to regulatory DNA sequences.[34]	MVATG18598 (pre-clinical), BCGΔureC::hly (VPM1002) (phase III) BCG AERAS-407 (pre-clinical)	*Mtb* / BCG
PPE18 (Rv1196)	Secreted protein involved in virulence and immune modulation.[33]	M72/AS01$_E$ (phase III), MTB72F-AS2A (phase I)	*Mtb*
PE13 (Rv1195)	Secreted protein with potential involvement on bacterial survival within macrophages.[33]	Pre-clinical data available, part of the TCR Informed TB AntigeN (TITAN) mRNA vaccine candidate.[35]	*Mtb* / BCG

Four customized multivalent mRNA constructs were generated, each encoding two antigens separated by a glycine-rich linker and preceded by a human IgE signal peptide. Constructs were formulated at equal ratios into sLNPs and administered as a single pulmonary booster following SC BCG vaccination (Fig. 3A). To broaden major histocompatibility complex (MHC) coverage, immunogenicity studies were performed in C57BL/6 × BALB/c F1 mice.

Flow cytometric analysis demonstrated that prime-and-pull vaccination (P&Px8) induced numbers of total $CD4^+$ T cells, $CD8^+$ T cells, and $CD4^+$ memory T cells in BALF, lung, and medLN that were comparable to those induced by SC BCG vaccination (Fig. 3B, E). In contrast, IT BCG induced substantially greater accumulation of T cells in all pulmonary compartments examined. Similarly, analysis of memory T cell subsets revealed higher numbers of T_{EM} and T_{RM}-like cells following

IT BCG vaccination, whereas the prime-and-pull regimen generated responses that were generally intermediate between SC and IT BCG vaccination (Fig. 3E)

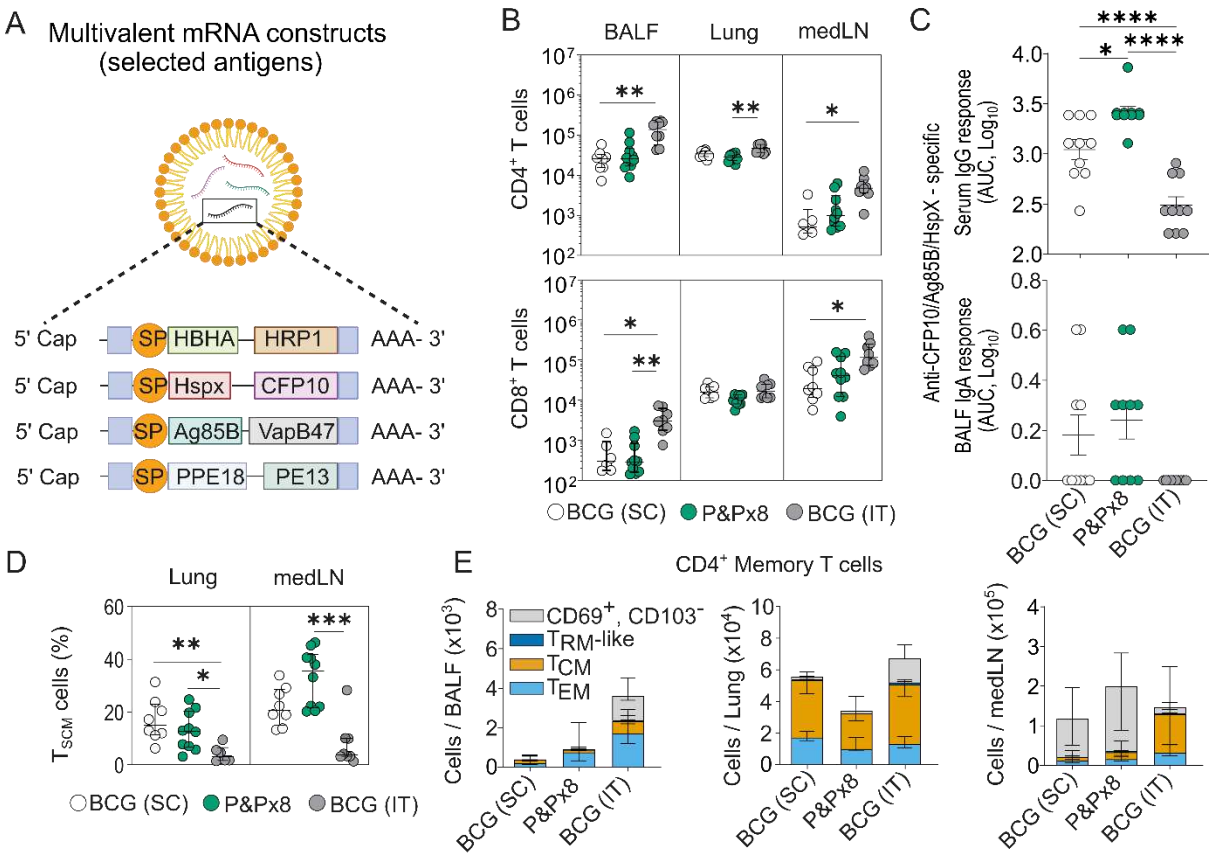


Figure 3. Immunogenicity of a multivalent mRNA prime-and-pull vaccination strategy. A. Schematic representation of the four multivalent mRNA constructs encoding eight selected *Mtb*- and BCG-derived antigens formulated in sLNPs. Hybrid F1 C57BL/6 × BALB/c mice were vaccinated with BCG either SC or IT as described previously. Prime-and-pull (P&Px8) mice received a single 10 µg pulmonary administration of the multivalent mRNA-sLNP formulation 14 days following SC BCG vaccination. Immune responses were analysed 28 days following primary vaccination. **B.** Number of $CD4^+$ and $CD8^+$ T cells in BALF, lungs, and medLN. **C.** Antigen-specific IgG and IgA responses in serum and BALF, respectively, quantified as area under the curve (AUC) from serial dilution ELISA measurements using a peptide mixture containing CFP10, Ag85B, and HspX epitopes. **D.** Percentage T_{SCM} cells in the lung and medLN. **E.** Number of $CD4^+$ memory T-cell populations, including $CD69^+CD103^-$ cells, T_{RM}-like cells, T_{CM} cells, and T_{EM} cells, in BALF, lungs, and medLN. Data were analysed using the Kruskal-Wallis test with Dunn's multiple-comparison post-test. NE = 2 independent experiments; *n* = 4-5 mice per group. Symbols represent individual animals and bars indicate the median and IQR. **P*<0.05, ***P*<0.01, ****P*<0.001, *****P*< 0.0001.

To assess antigen-specific responses, Ag85B-specific $CD4^+$ T cells were quantified using MHC-II tetramers. Similar numbers of Ag85B $tetramer^+$ T cells were detected following SC BCG and prime-and-pull vaccination, whereas IT BCG induced

significantly higher responses (Supp. Fig. 4A). No major differences in splenic T-cell populations were observed between groups (Supp. Fig. 4B-C). Because tetramer reagents were only available for Ag85B, antigen-specific responses to the remaining encoded proteins could not be directly assessed.

Antibody responses were evaluated against a peptide mixture containing CFP10, Ag85B, and HspX epitopes. Prime-and-pull vaccination induced significantly greater serum IgG reactivity than either SC or IT BCG vaccination (Fig. 3C). Antibody responses were quantified as area under the curve (AUC) from serial dilution ELISAs. Interpretation of CFP10-specific responses should be made with caution, as CFP10 is absent from BCG and therefore not expected to induce responses following BCG vaccination alone.

Stem cell-like memory T (T_{SCM}) cells are associated with long-term immune maintenance and the generation of secondary effector responses following antigen re-exposure.[36-41] Given the transient accumulation of pulmonary memory T cells observed following both prime-and-pull and IT BCG vaccination, we examined the frequency of T_{SCM} cells within the lung and medLN. Prime-and-pull vaccination was associated with significantly higher frequencies of T_{SCM} cells than IT BCG vaccination in both tissues (Fig. 3D).

Collectively, these findings indicate that pulmonary boosting with multi-antigen mRNA induces cellular immune responses comparable to those generated by SC BCG vaccination, while enhancing antibody reactivity and increasing T_{SCM} cell frequencies relative to IT BCG vaccination.

Prime-and-pull vaccination reduces bacterial burden and inflammatory responses following *Mtb* challenge

To evaluate protective efficacy, mice vaccinated with SC CG, prime-and-pull, or IT BCG were challenged with aerosolized *Mtb* 60 days following immunization. Two independent studies were performed using mRNA-sLNPs encoding either ESAT-6 or the multivalent antigen formulation.

In the ESAT-6 model, prime-and-pull vaccination reduced lung bacterial burden and pulmonary pathology compared with unvaccinated controls (Fig. 4A-C). The magnitude of protection was generally intermediate between SC and IT BCG::RD1 vaccination, mirroring the intermediate antigen-specific and memory T-cell responses observed following vaccination (Fig. 2). IT BCG::RD1 vaccination provided the greatest reduction in both bacterial burden and lung pathology (Fig. 4A–C).

In experiments using the multivalent mRNA formulation, all vaccination groups significantly reduced lung bacterial burden compared with unvaccinated controls (Fig. 4D). Comparable reductions were observed in mice receiving SC BCG and prime-and-pull vaccination, whereas IT BCG induced the greatest reduction in bacterial burden (approximately 18-fold relative to unvaccinated controls). Similar reductions in bacterial burden were also observed in the spleen, with the greatest reductions observed in IT BCG-vaccinated mice (Supp. Fig. 5). Differences in lung pathology were less pronounced, with significant reductions observed only in IT BCG-vaccinated animals (Fig. 4E, F).

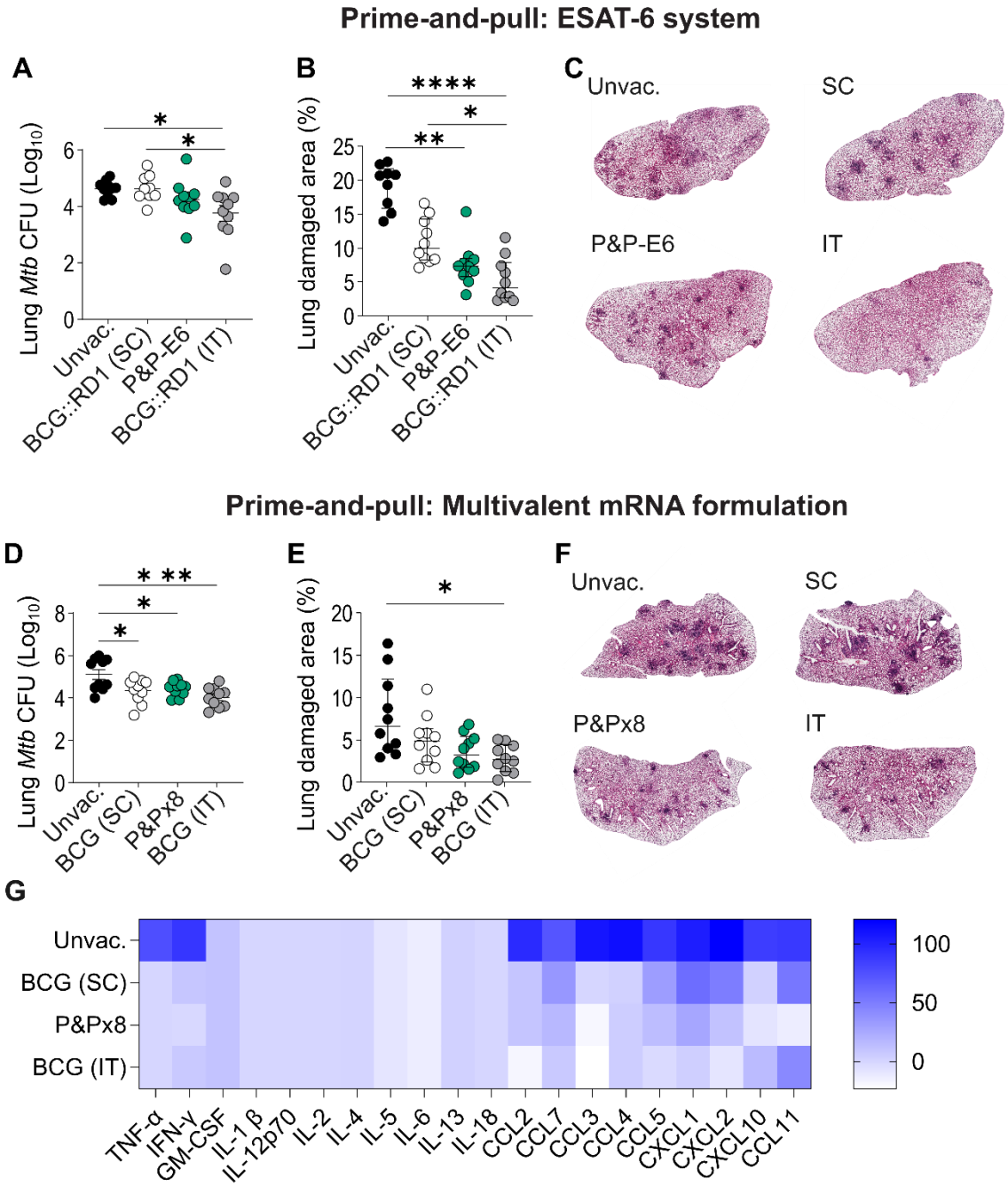


Figure 4. Prime-and-pull vaccination reduces bacterial burden following *Mtb* challenge and induces a lower inflammatory profile than intratracheal BCG vaccination. In **A-C**, C57BL/6 mice were vaccinated with BCG::RD1 either SC or IT. Prime-and-pull mice received a single 10 µg pulmonary administration of ESAT-6-mRNA-sLNPs 14 days following SC BCG::RD1 vaccination. In **D-G**, hybrid F1 C57BL/6 × BALB/c mice were vaccinated with BCG either SC or IT. Prime-and-pull (P&Px8) mice received a single 10 µg pulmonary administration of the multivalent mRNA-sLNP formulation 14 days following SC BCG vaccination. Sixty days after vaccination, mice were challenged by very low-dose aerosol infection with *Mtb* H37Rv. Bacterial burden and lung pathology were assessed 45 days post-infection. **ESAT-6 model: A.** Lung bacterial burden. **B.** Percentage of lung tissue area exhibiting dense inflammatory cellular infiltration. **C.** Representative H&E-stained lung sections. **Multivalent mRNA formulation: D.** Lung bacterial burden. **E.** Percentage of lung tissue area exhibiting dense inflammatory cellular infiltration. **F.** Representative H&E-stained lung sections. **G.** Serum cytokine and chemokine concentrations displayed as a heatmap of $\log_2$-transformed values. Bacterial burden data were $\log_{10}$-transformed and analysed using one-way ANOVA with Tukey's multiple-comparison post-test. Pathology data were analysed using the Kruskal-Wallis test with Dunn's multiple-comparison post-test. NE = 2 independent experiments; *n* = 5 mice per group. Symbols represent individual animals. For

bacterial burden analyses, bars indicate the mean ± SEM of log_{10}-transformed data. For pathology analyses, bars indicate the median and IQR. *P<0.05, **P<0.01, ***P<0.001, ****P< 0.0001.

Analysis of serum cytokine and chemokine concentrations demonstrated elevated inflammatory mediator levels in unvaccinated mice following infection, consistent with active disease (Fig. 4G). Vaccination was generally associated with reduced inflammatory signatures, with prime-and-pull and IT BCG groups exhibiting the lowest overall cytokine and chemokine concentrations.

Collectively, these findings demonstrate that prime-and-pull vaccination reduces bacterial burden following *Mtb* challenge and provides protection comparable to SC BCG vaccination, while maintaining a reduced inflammatory profile relative to unvaccinated animals.

Prime-and-pull vaccination induces local immune responses while limiting pulmonary inflammation

Finally, we directly compared inflammatory and immunological parameters across vaccination strategies. In the ESAT-6 model, IT BCG::RD1 induced the highest numbers of polyfunctional ESAT-6-specific IFN-γ^+TNF-α^+IL-2^+ $CD4^+$ and $CD8^+$ T cells in the lung (Fig. 5A). Prime-and-pull vaccination induced intermediate responses that were generally comparable to those observed following SC BCG::RD1 vaccination. Despite these differences in immunogenicity, IT BCG::RD1 vaccination was associated with substantially greater pulmonary pathology 4 weeks after vaccination, whereas prime-and-pull and SC BCG::RD1 vaccination induced similarly low levels of lung damage (Fig. 5B).

A similar pattern was observed with the multivalent mRNA formulation. Prime-and-pull vaccination induced lower inflammatory responses than IT BCG vaccination while maintaining local immune responses comparable to those induced by SC BCG vaccination (Fig. 5D). Furthermore, pulmonary pathology following prime-and-pull vaccination remained markedly lower than that observed following IT BCG vaccination (Fig. 5E).

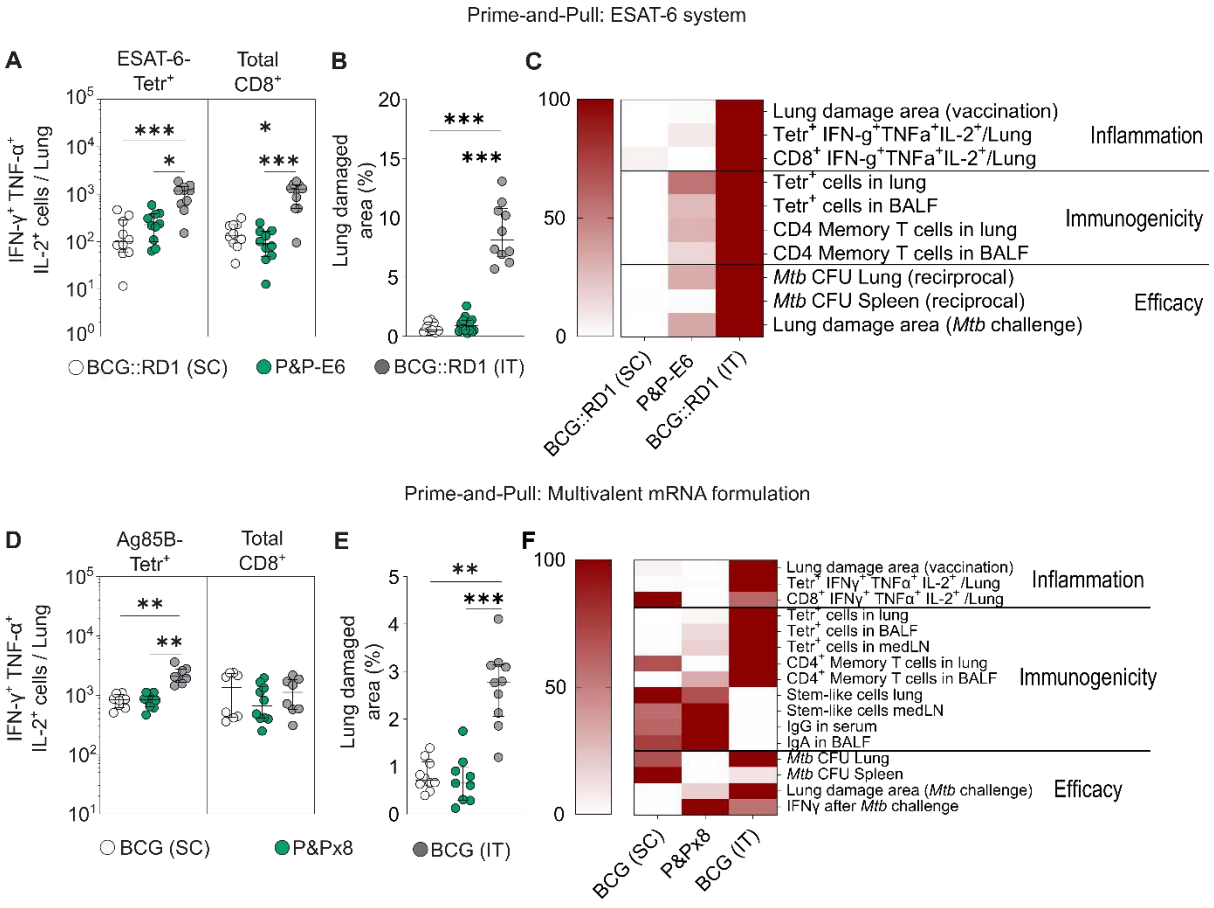


Figure 5. Prime-and-pull vaccination induces local immune responses while limiting pulmonary inflammation. A-C. Data from the ESAT-6 model. **D-F.** Data from the multivalent mRNA formulation. Mice were vaccinated as described in Fig. 2 and Fig. 3, respectively. Cytokine producing T cell and pulmonary pathology were assessed 28 days following vaccination. **ESAT-6 model: A.** Number of lung ESAT-6 tetramer$^+$ and total CD8$^+$ T cells producing IFN-γ, TNF-α, and IL-2. **B.** Percentage of lung tissue area exhibiting dense inflammatory cellular infiltration 4 weeks following vaccination. **C.** Integrated heatmap summarizing inflammatory, immunological, and protection-associated parameters. **Multivalent mRNA formulation: D.** Number of lung Ag85B tetramer$^+$ and total CD8$^+$ T cells producing IFN-γ, TNF-α, and IL-2. **E.** Percentage of lung tissue area exhibiting dense inflammatory cellular infiltration 4 weeks following vaccination. **F.** Integrated heatmap summarizing inflammatory, immunological, and protection-associated parameters. Data were analysed using the Kruskal-Wallis test with Dunn's multiple-comparison post-test. NE = 2-3 independent experiments; *n* = 4-5 mice per group. Symbols represent individual animals and bars indicate the median and IQR. **P*<0.05, ***P*<0.01, ****P*<0.001, *****P*< 0.0001.

To facilitate integrated visualization of inflammatory, immunological, and protection-associated parameters, normalized heatmaps were generated for the ESAT-6 system and the multivalent mRNA formulation (Fig. 5C & 5F). These heatmaps support the overall trend observed throughout the study, with prime-and-pull vaccination exhibiting a lower inflammatory profile than IT BCG vaccination while maintaining local immune responses comparable to those induced by IT BCG vaccination.

Collectively, these findings indicate that pulmonary mRNA boosting following BCG priming promotes local immune responses while limiting the pulmonary pathology associated with intratracheal BCG vaccination.

Discussion

The development of improved vaccines and alternative vaccination strategies remains central to achieving TB reduction, elimination, and ultimately eradication in line with WHO goals. Here, we demonstrate that a prime-and-pull vaccination strategy can enhance local pulmonary immune responses while limiting the inflammatory burden associated with pulmonary BCG vaccination. By combining systemic BCG priming with pulmonary mRNA delivery, this approach increased antigen-specific and memory T cell responses within the lung and mediastinal lymph nodes while causing substantially less histopathological damage than intratracheal BCG vaccination. In addition, inclusion of an mRNA-only control demonstrated that pulmonary mRNA administration following BCG priming generated greater antigen-specific T cell responses than either intervention alone, consistent with a prime-and-pull effect. Together, these findings establish proof-of-concept for an mRNA-based strategy to augment local pulmonary immunity following conventional BCG vaccination.

A major advantage of this approach is its ability to promote local immune responses while limiting vaccine-associated pulmonary inflammation. Because the lung is highly susceptible to immunopathology, respiratory vaccines must balance immune activation with preservation of tissue integrity and function.[42,43] Chronic or excessive inflammation can impair vaccine efficacy and contribute to pulmonary pathology.[44-47] Consistent with our previous observations that pulmonary BCG and BCG::RD1 vaccination induce moderate and severe lung pathology, respectively,[48] prime-and-pull vaccination induced antigen-specific and memory T-cell responses, including T cell populations expressing tissue-residency markers, while maintaining low levels of pulmonary pathology. These findings suggest that enhancement of local pulmonary immunity can be achieved without the degree of inflammation associated with pulmonary administration of live mycobacteria.

The use of sLNPs for mucosal delivery is a key component of this platform. Conventional mRNA-LNP formulations have largely been optimised for intramuscular delivery and show limited efficacy when administered via the respiratory tract. [49-51] In contrast, pulmonary administration of sLNP-formulated mRNA supported transgene expression in multiple pulmonary cell populations and increased antigen-specific and memory T cell responses following BCG priming. These observations are consistent with previous studies demonstrating enhanced pulmonary immunity following respiratory delivery of mRNA vaccines.[51,52] Together, our findings support the potential utility of sLNPs as a platform for pulmonary mRNA vaccination.

The growing body of evidence supporting mRNA vaccination for TB also highlights the importance of vaccine delivery strategy. Multivalent LNP-formulated mRNA vaccines

have been shown to induce antigen-specific Th1 and $CD8^+$ T-cell responses and confer protection against *Mtb* challenge, although systemic mRNA boosting did not further enhance BCG-mediated protection.[53] Likewise, intramuscular mRNA vaccination has been reported to augment BCG-induced immunity through the induction of polyfunctional Th1 responses and modulation of innate immune pathways.[54] More recently, heterologous vaccination strategies combining systemic and respiratory immunization have been shown to promote lung-resident immune responses and improve protection, reinforcing the importance of directing vaccine-induced immunity to the respiratory tract.[55]

Our findings extend this emerging body of work by demonstrating that mRNA can serve as the pulmonary component of a prime-and-pull vaccination strategy when delivered using sLNPs. Unlike approaches that rely on viral vectors to recruit immune cells into the lung, pulmonary delivery of mRNA-sLNPs enhanced local antigen-specific and memory T cell responses following BCG priming while inducing substantially less pulmonary inflammation than intratracheal BCG vaccination. Collectively, these studies suggest that the success of mRNA-based TB vaccination may depend not only on antigen selection but also on developing delivery strategies capable of promoting immune responses at the site of infection.

An additional feature of the prime-and-pull strategy was the increased frequency of T_{SCM} cells in the lung and medLN. These cells provide a self-renewing reservoir capable of replenishing effector and memory T cell populations following antigen re-encounter, potentially contributing to the maintenance of long-term immunity. [36,38] Although the functional significance of these cells was not directly assessed in the

present study, the increased T_{SCM} cell frequencies observed following prime-and-pull vaccination suggest that pulmonary mRNA boosting may support the establishment of durable memory responses. Future studies incorporating longer follow-up periods will be required to determine whether these immunological differences translate into improved long-term protection.

The multivalent mRNA formulation also broadened humoral immune responses, increasing serum IgG reactivity against CFP10, Ag85B, and HspX compared with both SC and IT BCG vaccination. Because antibody responses were quantified using a peptide mixture containing these three antigens, interpretation should be restricted to the antigens directly assessed. The eight encoded antigens were selected based on evidence of immune recognition in humans and mice, expression during *Mtb* infection, the presence of T and B cell epitopes, and previous incorporation into TB vaccine candidates. Encoding full-length antigens may facilitate presentation of multiple epitopes across diverse HLA class I and II backgrounds, potentially increasing the breadth of vaccine-induced immune responses. Nevertheless, the multivalent formulation should be viewed as an approach to maximise antigenic diversity rather than as a definitive clinical vaccine composition, as the optimal antigen combination for broad protection remains unknown. Accordingly, the present study establishes proof-of-concept for a multivalent pulmonary mRNA boosting strategy, rather than defining the final antigen composition required for clinical translation.

Translation of this approach will require further optimization of both antigen delivery and vaccine formulation. Intratracheal administration was used in the present study to ensure precise and reproducible dosing in mice; however, aerosolized or intranasal

485 delivery would likely be more practical for clinical implementation.[56,57] Advances in lipid
486 nanoparticle engineering further support this possibility, as modifications to lipid
487 composition and surface characteristics can influence tissue tropism and facilitate
488 enhanced pulmonary delivery.[58,59] In our study, sLNPs supported pulmonary mRNA
489 expression and were associated with limited vaccine-induced inflammation,
490 suggesting their suitability as a platform for respiratory mRNA vaccination. We also
491 observed evidence of dose-dependent immune responses, with a single 10 μg
492 administration outperforming repeated lower-dose regimens. This finding is consistent
493 with reports demonstrating that repeated LNP administration can induce innate
494 immune sensing and type I interferon responses that may reduce the effectiveness of
495 subsequent doses.[60,61] Future development of this approach may therefore benefit
496 from dose-sparing technologies, including self-amplifying RNA platforms, which could
497 prolong antigen expression while reducing the amount of input RNA required.[58-60]
498
499 An important feature of the prime-and-pull strategy is that it builds upon, rather than
500 replaces, conventional BCG vaccination. In addition to providing protection against
501 TB, BCG has been associated with heterologous immunological effects that may
502 reduce susceptibility to unrelated infectious diseases. Meta-analyses of randomized
503 studies in Guinea-Bissau reported reductions in infant and neonatal mortality following
504 BCG vaccination,[62-64] while a randomized trial in India demonstrated reductions in both
505 all-cause neonatal mortality and infection-related mortality.[65] These effects are thought
506 to result, at least in part, from the induction of trained immunity through epigenetic and
507 metabolic reprogramming of innate immune cells.[66-68] By preserving systemic BCG
508 vaccination while selectively enhancing pulmonary immune responses, the prime-and-

509 pull strategy seeks to retain these established benefits while targeting immunity to the
510 primary site of *Mtb* infection and transmission.
511
512 Several limitations should be acknowledged. Although prime-and-pull vaccination
513 increased stem cell-like memory T cell populations, longer-term studies will be
514 required to determine whether these responses translate into durable protection. The
515 antigen-specificity of the multivalent formulation was only partially resolved, as Ag85B-
516 specific tetramers and antibody responses against CFP10, Ag85B, and HspX
517 represented the only antigen-specific readouts available. Furthermore, murine models
518 cannot fully reproduce the complexity of human TB, including granuloma formation,
519 latency, and reactivation.[69] Finally, although the multivalent construct targeted eight
520 immunodominant antigens, further optimisation of antigen selection and formulation
521 will likely be required before clinical translation.
522
523 In conclusion, we demonstrate that a prime-and-pull vaccination strategy can enhance
524 local pulmonary immune responses while limiting the inflammatory burden associated
525 with pulmonary BCG vaccination. By combining systemic BCG priming with pulmonary
526 delivery of a multivalent mRNA formulation in sLNPs, this approach increased antigen-
527 specific immune responses in the lung with substantially less pulmonary pathology
528 than IT BCG vaccination. Protection following *Mtb* challenge was comparable to that
529 achieved by SC BCG vaccination, while evidence from the ESAT-6 model supported
530 a prime-and-pull effect in the generation of local antigen-specific T cell responses.
531 Together, these findings establish proof-of-concept for an adaptable pulmonary mRNA
532 boosting strategy that may complement conventional BCG vaccination and inform the
533 development of next-generation TB vaccines.

Materials and methods

Bacterial strains and culture conditions

Mycobacterium bovis BCG SSI Danish (hereafter referred to as BCG), recombinant BCG expressing the *Mtb* ESX 1 locus (BCG::ESX1^{Mtb}, also referred to as BCG::RD1), and *Mtb* H37Rv were cultured in Middlebrook 7H9 broth (BD Difco) supplemented with 10% oleic albumin dextrose catalase (OADC; USBiological Life Sciences), 0.05% Tween-80, 0.2% glycerol, and appropriate antibiotics at 37°C until mid-logarithmic phase, harvested, and stored in sterile PBS containing 15% glycerol at −80°C until use.

mRNA molecules

Commercial reporter mRNA encoding enhanced green fluorescent protein (ARCA-EGFP mRNA, 5-moUTP) was purchased from APExBIO. All custom mRNA constructs were obtained from Messenger Bio (https://www.messenger.bio/mrna). These constructs included N1-methylpseudouridine modifications, Cap1 capping, optimized 5′ and 3′ untranslated regions, and a 100-nt poly(A) tail. Codon optimization for mammalian expression was performed as part of the Messenger Bio service.

For proof-of-concept studies, mRNA encoding ESAT-6 was generated. For subsequent experiments, four multi-antigen mRNA constructs were designed using the general architecture signal peptide (SP)–antigen 1–linker–antigen 2. Coding sequences for the selected antigens were obtained from the Mycobrowser database (https://mycobrowser.epfl.ch).

The multi-antigen constructs were as follows:

- Molecule 1, SP–HBHA–linker–HRP1 (1101 nt).
- Molecule 2, SP–HspX–linker–CFP10 (807 nt).
- Molecule 3, SP–Ag85B–linker–VapB47 (1347 nt).
- Molecule 4, SP–PPE18–linker–PE13 (1542 nt).

The human IgE signal peptide sequence was *atggattggacctggattctgtttctggtggcggcggcgacccgcgtgcatagc*, and the linker sequence was *agggcggcggcggcagc*.

All mRNA constructs were mixed in equal amounts (250 µg each), aliquoted into two portions, and stored at -80°C before formulation.

Lipid nanoparticle formulation:

mRNA constructs were formulated into “stealth” lipid nanoparticles (sLNPs) by the Griffith University Nanomedicine Biofoundry using a hydration of freeze-dried matrix method (HFDM), based on a previously described formulation.[24] Briefly, the required amounts of each lipid and C16 PEG-ceramide were mixed with the mRNA at an N:P ratio of 6 in a sucrose-containing water/tert-butanol (1:1, v/v) co-solvent system. DOTAP, DOPE, cholesterol, and C16 PEG-ceramide were used at a molar ratio of 50:5:35:10, respectively. The formulation was prepared at pH 7.5, with tert-butanol removed by sublimation during the HFDM process. The resulting mRNA-sLNPs were prepared in an aqueous sucrose matrix (92.5 mg/mL), snap-frozen, and lyophilized. Lyophilized mRNA-sLNPs were stored at −80°C for up to six months.

Prior to use, lyophilized mRNA-sLNPs were equilibrated to room temperature for 30 min and rehydrated with nuclease-free water (Thermo Fisher Scientific) to a final mRNA concentration of 0.2 µg/µL. Samples were gently swirled, incubated at room

584 temperature for 2 h, and stored at 4°C for up to 48 h before *in vivo* administration.
585 Particle size and polydispersity index (PDI) were determined by dynamic light
586 scattering (DLS) using a Zetasizer Nano ZS (Malvern Instruments, Malvern, UK).
587 mRNA encapsulation efficiency was determined using a RiboGreen assay (Thermo
588 Fisher Scientific). Quality control analysis of representative batches indicated a mean
589 particle diameter of approximately 200 nm and an encapsulation efficiency of 97%.
590
591 **Mice**
592 Female C57BL/6 mice (6–8 weeks old) were obtained from the Animal Resource
593 Centre (Perth, Australia) for GFP and ESAT-6 proof-of-concept experiments. For
594 multi-antigen prime-and-pull studies, female C57BL/6 × BALB/c F1 hybrid mice were
595 bred and maintained in-house. All animals were acclimatized for at least one week
596 prior to experimentation and housed under specific pathogen-free conditions in
597 biosafety level 2 or 3 facilities at the Australian Institute of Tropical Health and
598 Medicine (AITHM), James Cook University. All procedures were conducted in
599 accordance with National Health and Medical Research Council (NHMRC) guidelines
600 and approved by the James Cook University Animal Ethics Committee (approval no.
601 A2837).
602
603 **Vaccination protocols**
604 Frozen BCG stocks were thawed, washed, sonicated, and diluted in sterile PBS prior
605 to immunization. Mice were immunised either subcutaneously (SC; 1×10^6 CFU in
606 100 µL) or intratracheally (IT; 1×10^5 CFU in 50 µL). For prime-and-pull vaccination,
607 mice were primed with the specified BCG strain SC on day 0, followed by IT
608 administration of mRNA-sLNPs according to the schedules described below.

For the ESAT-6 proof-of-concept studies, mice received either a single 5 μg mRNA-sLNP dose on day 14 (P&P-E6 [5 μg × 1]), two 5 μg doses on days 7 and 14 (P&P-E6 [5 μg × 2]), three 5 μg doses on days 7, 14, and 21 (P&P-E6 [5 μg × 3]), or a single 10 μg dose on day 14 (P&P-E6 [10 μg × 1]). The mRNA-only control group received a single 5 μg dose of mRNA-sLNPs IT on day 14 without prior BCG vaccination. For the multivalent experiments, prime-and-pull vaccinated mice received BCG SC on day 0, followed by a single IT administration of 10 μg mRNA-sLNPs. Detailed vaccination schedules and doses for individual experiments are provided in the corresponding figure legends.

For IT administration, mice were anesthetized with isoflurane and suspended by the upper incisors from a metal support using a hanging wire. The tongue was gently displaced laterally using forceps to allow direct visualization of the trachea. A 200 μL pipette was used to administer 50 μL of BCG or mRNA-sLNP formulation directly into the trachea. Following administration, the tongue was released, and animals were observed for a gag reflex indicative of delivery into the airway. Mice were then gently returned to their cages with the airways unobstructed and monitored until recovery, which typically occurred within approximately 3 min.

Mtb challenge and bacterial burden and histopathological analysis

Sixty days after primary vaccination, mice were challenged by aerosol exposure to *Mtb* H37Rv using a Glas-Col inhalation exposure system, resulting in implantation of approximately 10-70 CFU per mouse. At 45 days post-challenge, mice were euthanized, and lungs and spleens were aseptically collected. Organs were homogenized in sterile PBS containing Tween-80, serially diluted, and plated on

Middlebrook 7H11 agar supplemented with OADC. Colonies were enumerated following incubation at 37°C for 5-8 weeks. Bacterial burden is reported as log10 CFU per organ.

For histopathological analysis, lung lobes were fixed in 10% neutral-buffered formalin, embedded in paraffin, sectioned (4 µm), and stained with haematoxylin and eosin (H&E). Whole-slide images were acquired using an Aperio CS2 scanner and analysed using Aperio ImageScope and ImageJ software. Pulmonary pathology was quantified as the percentage of lung tissue area exhibiting dense inflammatory cellular infiltration.

Tissue processing and cell preparation

At 4 or 8 weeks following BCG immunization, bronchoalveolar lavage fluid (BALF), lungs, mediastinal lymph nodes (medLN), and spleens were collected for analysis. BALF was obtained by lavage of the airways with sterile PBS. Cells were recovered by centrifugation, subjected to erythrocyte lysis where required, washed in FACS buffer, and processed for flow cytometric analysis. BALF supernatants were stored at −80°C for antibody measurements.

Prior to lung collection, mice were perfused via the right ventricle with sterile PBS to remove circulating blood cells from the pulmonary vasculature. Lungs were mechanically dissociated using a GentleMACS™ Dissociator (Miltenyi Biotec) and enzymatically digested in RPMI containing collagenase D (7.5 µg/mL), collagenase VIII (1.75 µg/mL), and DNase I (200 µg/mL) (all Sigma-Aldrich) for 30 min at 37°C. Digested tissues were passed through 70-µm cell strainers to generate single-cell

suspensions. Following erythrocyte lysis, cells were washed and resuspended in FACS buffer.

Spleens and medLN were mechanically dissociated through 70-µm cell strainers to obtain single-cell suspensions. Splenocytes were subjected to erythrocyte lysis before washing and resuspension in FACS buffer.

Cell surface and intracellular cytokine staining

Single-cell suspensions prepared from spleen, lung, and medLN were cultured in complete RPMI medium in the presence or absence of Cell Stimulation Cocktail (2 µL/mL; eBioscience, 00-4975-93) and brefeldin A (BD Biosciences, 555029) for 5-6 h at 37°C in a humidified incubator containing 5% CO_2.

Dead cells were excluded using Horizon™ Fixable Viability Stain 780 (BD Biosciences). For surface staining, cells were incubated with antibodies against TCRβ (BUV737, clone H57-597), CD8α (AF800, clone 53-6.7), CD4 (BUV395, clone GK1.5), CD44 (BV421, clone IM7), CD69 (PE-CF594, clone H1.2F3), CD103 (BV710, clone M290), CD11c (BUV395, clone HL3), I-A/I-E (BV711, clone M5/114), CD45.2 (BV650, clone 104), CD64 (BV786, clone X54-5/7.1) (all BD Horizon); CD62L (PE-Cy7, clone MEL-14), MerTK (BV421, clone 2B10C42), CD3 (BV510, clone 17A2), Ly-6G (PerCP-Cy5.5, clone 1A8), and CD11b (PE-Cy7, clone M1/70) (all BioLegend); and Siglec-F (PE, clone E50-2440), EpCAM/CD326 (APC, clone 9C4), and SLAMF-6 (PE, clone 13G3) (BD Pharmingen).

MHC-II tetramer monomers specific for I-A^b ESAT-6_{4-17} and I-A^b Ag85$B_{280-294}$ were obtained from the NIH Tetramer Core Facility (Emory University, Atlanta, GA, USA).

683 Tetramers were generated in-house by conjugation with streptavidin-APC (Thermo
684 Fisher Scientific).
685
686 Following surface staining, cells were fixed and permeabilized using the Intracellular
687 Fixation and Permeabilization Buffer Set (Invitrogen, 88-8824-00) according to the
688 manufacturer's instructions. Intracellular staining was performed using antibodies
689 against IFN-γ (PerCP-Cy5.5, clone XMG1.2), TNF-α (PE, clone MP6-XT22)
690 (BioLegend), IL-2 (BV605, clone JES6-5H4), and TCF-1 (BV421, clone S33-966) (BD
691 Horizon).
692
693 Cell populations were defined as follows: neutrophils (Neut) (Ly-6^{Hi}CD11b^{Hi}), dendritic
694 cells (DC) (Ly-6G$^{-/+}$MerTK^{-}Siglec-F^{-}CD11c^{+}I-A/I-E^{+}), interstitial macrophages (IM) (Ly-
695 6G$^{-/+}$MerTK^{+}CD64^{+}SIglec-F^{-}), alveolar macrophages (AM) (Ly-6G^{-}
696 $^{/+}$MerTK^{+}CD64^{+}SIglec-F^{+}). Representative gating strategies are shown in
697 Supplementary Fig. 1. Effector memory T (T_{EM}) cells (CD44^{+}CD62L^{-}CD69^{-}CD103^{-}),
698 central memory T (T_{CM}) cells (CD44^{+}CD62L^{+}), CD69^{+}CD103^{-} memory T cells
699 (CD44^{+}CD62L^{-}CD69^{+}CD103^{-}), stem cell-like memory T cells (TCRβ^{+}KLRG1^{-}TCF-1^{+}).
700 [70] Cells expressing both CD69 and CD103 were designated T_{RM}-like cells
701 (CD44^{+}CD62L^{-}CD69^{+}CD103^{+}) based on expression of canonical tissue-residency
702 markers; intravascular staining was not performed.
703
704 Samples were acquired on a BD LSRFortessa X-20 cytometer using FACSDiva
705 software (BD Biosciences). The data were analysed by FlowJo software, versions 9
706 and 10 (Treestar). Absolute cell numbers were calculated using counting beads.
707

ELISA

Blood was collected into Z-gel tubes (Sarstedt) and centrifuged at 8,000 rpm for 8 min to obtain serum, which was stored at −80°C until analysis. Antigen-specific IgG and IgA responses were measured in serum and BALF, respectively, by ELISA.

A peptide mixture containing $Rv3874_{76\text{-}90}$ (CFP10), $Rv1886c_{280\text{-}294}$ (Ag85B) and $Rv2031c_{280\text{-}294}$ (HspX) was used as coating antigen. Costar 96 well plates (Corning, USA, 3590) were coated with the peptide mixture in carbonate coating buffer for 8 h at room temperature, washed with PBS containing 0.05% Tween-20 (PBST), and blocked overnight at 4°C with 5% skim milk in PBST. Following four washes with PBST, diluted serum or BALF samples were added in 0.5% skim milk-PBST and incubated in a humidified chamber at 37°C. Plates were washed again and incubated for 2 h at 37°C biotinylated goat anti-mouse IgG (1:3000; Sigma, SAB4600004) or biotinylated goat anti-mouse IgA (1:1000; BD Biosciences, 556978).

After washing, plates were incubated with HRP-conjugated streptavidin (1:1000; BD Biosciences, 554066) for 1 h at 37°C. Bound antibodies were detected using TMB substrate (BD Biosciences, 555214) for 20 min at room temperature in the dark. Reactions were stopped with 0.18 M H_2SO_4 and absorbance was measured at 450 nm using a POLARstar Omega plate reader (BMG Labtech).

Antibody responses were quantified from serial sample dilutions by calculating the area under the curve (AUC) of the dilution-response relationship.

Serum cytokine and chemokine analysis

Frozen serum samples were thawed on ice and prepared according to the manufacturer's instructions for the Bio-Plex Pro™ Mouse Cytokine 23-Plex Assay (Bio-Rad). Samples were analysed in duplicate using a MAGPIX® instrument (Luminex), and cytokine and chemokine concentrations were determined from standard curves generated for each analyte according to the manufacturer's recommendations.

For analytes with concentrations below the limit of detection, the lowest detectable value for the respective analyte was assigned for downstream analysis and visualization. Cytokine and chemokine concentrations were log2-transformed and displayed as heatmaps generated using GraphPad Prism.

Statistics

Statistical analyses were performed using GraphPad Prism 8 or 9 (GraphPad Software). Comparisons between multiple groups were performed using Kruskal-Wallis tests with Dunn's multiple-comparison post-test or one-way ANOVA with Tukey's multiple-comparison post-test, as indicated in the respective figure legends.

Bacterial burden data were log10-transformed prior to analysis by one-way ANOVA. Cytokine and chemokine concentrations were log2-transformed for heatmap visualization.

Integrated heatmaps presented in Figure 5 were generated using median values from each vaccination group. Parameters were normalized independently by assigning the

minimum value to 0 and the maximum value to 100 to facilitate visualization and comparison across datasets. For protection-associated parameters, reciprocal values were used where appropriate such that higher values consistently reflected more favourable outcomes. Parameters included vaccination-associated pulmonary pathology, antigen-specific and polyfunctional T-cell responses, memory T-cell responses, antibody responses (where applicable), cytokine and chemokine responses following *Mtb* challenge, and protection-associated outcomes. Heatmaps are presented as an integrated visualization of trends observed throughout the study and were not used for statistical inference.

Contributors

Conceptualization: AK, AMVH. Methodology: AK, AMVH. Investigation: AMVH, GZ, JS, HDS, SMH, MP. Manuscript writing: AMVH, AK. Funding acquisition: AK, AMVH.

Declaration of Interests

The authors declare no competing interests.

Acknowledgements

We acknowledge the NanoMedicine Biofoundry (Institute for Biomedicine and Glycomics, Griffith University) for the design, formulation, and supply of the LNP materials used. We also acknowledge the NIH Tetramer Core Facility for kindly providing monomers and instructions for tetramerization.

Data Sharing Statement

All data are available in the main text or the supplementary materials. Requests for further information and resources should be directed to and will be fulfilled by the lead contact.

Funding

This work was supported by the NHMRC Investigator Grant (APP2008715) and the James Cook University Women's Parental Leave Continuity Grant.

Clinical trial number

Not applicable

Consent to Participate

Not applicable

Artificial intelligence (AI) disclosure

Generative artificial intelligence (Microsoft Copilot) was used to assist with language editing and manuscript refinement. The authors reviewed and edited all AI-generated content and accept full responsibility for the content of the publication.

References

1 Arts, R. J. W. *et al.* BCG Vaccination Protects against Experimental Viral Infection in Humans through the Induction of Cytokines Associated with Trained Immunity. *Cell Host and Microbe* **23**, 89-100.e105 (2018). https://doi.org/10.1016/j.chom.2017.12.010

2 Dockrell, H. M. & Smith, S. G. in *Frontiers in Immunology* Vol. 8 (Frontiers Media S.A., 2017).

3 Lalvani, A. & Sridhar, S. BCG vaccination: 90 years on and still so much to learn. *Thorax* **65**, 1036-1038 (2010). https://doi.org/10.1136/thx.2010.140897

4 Stensballe, L. G. *et al.* Acute lower respiratory tract infections and respiratory syncytial virus in infants in Guinea-Bissau: A beneficial effect of BCG

vaccination for girls: Community based case-control study. *Vaccine* **23**, 1251-1257 (2005). https://doi.org/10.1016/j.vaccine.2004.09.006

5 Walk, J. *et al.* Outcomes of controlled human malaria infection after BCG vaccination. *Nature Communications* **10** (2019). https://doi.org/10.1038/s41467-019-08659-3

6 Baily, G. V. Tuberculosis prevention Trial, Madras. *The Indian journal of medical research* **72 Suppl**, 1-74 (1980).

7 Comstock, G. W., Woolpert, S. F. & Livesay, V. T. Tuberculosis studies in Muscogee County, Georgia. Twenty-year evaluation of a community trial of BCG vaccination. *Public health reports (Washington, D.C. : 1974)* **91**, 276-280 (1976).

8 Fourth Report to the Medical Research Council by its Tuberculosis Vaccines Clinical Trials, C. BCG and vole bacillus vaccines in the prevention of tuberculosis in adolescence and early adult life. *Bulletin of the World Health Organization* **46**, 371-385 (1972).

9 Ponnighaus, J. M. *et al.* Efficacy of BCG vaccine against leprosy and tuberculosis in northern Malawi. *The Lancet* **339**, 636-639 (1992). https://doi.org/10.1016/0140-6736(92)90794-4

10 Shapiro, C. *et al.* A Case-Control Study of BCG and Childhood Tuberculosis in Cali, Colombia. (1985).

11 Tverdal, A. & Funnemark, E. Protective effect of BCG vaccination in Norway 1956–1973. *Tubercle* **69**, 119-123 (1988). https://doi.org/10.1016/0041-3879(88)90074-8

12 Torracinta, L., Nassanga, B. & Tanner, R. in *Tuberculosis Vaccines* 97-131 (Springer Nature Switzerland, 2025).

13 Boraschi, D. *et al.* Advocating mucosal immunization: A global need in a viewpoint from China. *The Innovation* **6**, 100951-100951 (2025). https://doi.org/10.1016/j.xinn.2025.100951

14 Miquel-Clopés, A., Bentley, E. G., Stewart, J. P. & Carding, S. R. Mucosal vaccines and technology. *Clinical and Experimental Immunology* **196**, 205-214 (2019). https://doi.org/10.1111/cei.13285

15 Zhang, H. *et al.* Mucosal vaccination in mice provides protection from diverse respiratory threats. *Science* (2026). https://doi.org/10.1126/science.aea1260

16 Audran, R. *et al.* Randomised, double-blind, controlled phase 1 trial of the candidate tuberculosis vaccine ChAdOx1-85A delivered by aerosol versus intramuscular route. *Journal of Infection* **89** (2024). https://doi.org/10.1016/j.jinf.2024.106205

17 Jeyanathan, M. *et al.* Aerosol delivery, but not intramuscular injection, of adenovirus-vectored tuberculosis vaccine induces respiratorymucosal immunity in humans. *JCI Insight* **7** (2022). https://doi.org/10.1172/jci.insight.155655

18 Manjaly Thomas, Z. R. *et al.* Alternate aerosol and systemic immunisation with a recombinant viral vector for tuberculosis, MVA85A: A phase I randomised controlled trial. *PLoS Medicine* **16** (2019). https://doi.org/10.1371/journal.pmed.1002790

19 Satti, I. *et al.* Safety and immunogenicity of a candidate tuberculosis vaccine MVA85A delivered by aerosol in BCG-vaccinated healthy adults: A phase 1, double-blind, randomised controlled trial. *The Lancet Infectious Diseases* **14**, 939-946 (2014). https://doi.org/10.1016/S1473-3099(14)70845-X

20 Stosman, K. I., Aleksandrov, A. G., Sivak, K. V., Buzitskaya, Z. V. & Stukova, M. A. Evaluation of the immunotoxicity and allergenicity of a new intranasal influenza vector vaccine against tuberculosis carrying TB10.4 and HspX antigens. *Iranian journal of basic medical sciences* **26**, 558-563 (2023). https://doi.org/10.22038/IJBMS.2023.68440.14936

21 Fredsgaard-Jones, T. *et al.* A dose escalation study to evaluate the safety of an aerosol BCG infection in previously BCG-vaccinated healthy human UK adults. *Frontiers in Immunology* **15** (2024). https://doi.org/10.3389/fimmu.2024.1427371

22 Idris, A. *et al.* A SARS-CoV-2 targeted siRNA-nanoparticle therapy for COVID-19. *Molecular Therapy* **29**, 2219-2226 (2021). https://doi.org/10.1016/j.ymthe.2021.05.004

23 McCaskill, J. *et al.* Efficient biodistribution and gene silencing in the lung epithelium via intravenous liposomal delivery of siRNA. *Molecular Therapy - Nucleic Acids* **2** (2013). https://doi.org/10.1038/mtna.2013.22

24 Wu, S. Y. *et al.* Development of a Novel Method for Formulating Stable siRNA-Loaded Lipid Particles for In vivo Use. *Pharmaceutical Research* **26**, 512-522 (2009). https://doi.org/10.1007/s11095-008-9766-1

25 Perdomo, C. *et al.* Mucosal BCG vaccination induces protective lung-resident memory T cell populations against tuberculosis. *mBio* **7**, 1-11 (2016). https://doi.org/10.1128/mBio.01686-16

26 Muruganandah, V. *et al.* A systematic approach to simultaneously evaluate safety, immunogenicity, and efficacy of novel tuberculosis vaccination strategies. (2020).

27 Pym, A. S., Brodin, P., Brosch, R., Huerre, M. & Cole, S. T. Loss of RD1 contributed to the attenuation of the live tuberculosis vaccines Mycobacterium bovis BCG and Mycobacterium microti. *Molecular Microbiology* **46**, 709-717 (2002). https://doi.org/10.1046/j.1365-2958.2002.03237.x

28 Pethe, K. *et al.* Mycobacterial heparin-binding hemagglutinin and laminin-binding protein share antigenic methyllysines that confer resistance to proteolysis. *Proceedings of the National Academy of Sciences* **99**, 10759-10764 (2002). https://doi.org/10.1073/pnas.162246899

29 Wang, J. *et al.* A VLP-Based Vaccine Displaying HBHA and MTP Antigens of Mycobacterium tuberculosis Induces Protective Immune Responses in M. tuberculosis H37Ra Infected Mice. *Vaccines* **11** (2023). https://doi.org/10.3390/vaccines11050941

30 Rosenkrands, I. *et al.* Hypoxic response of Mycobacterium tuberculosis studied by metabolic labeling and proteome analysis of cellular and extracellular proteins. *Journal of bacteriology* **184**, 3485-3491 (2002). https://doi.org/10.1128/JB.184.13.3485-3491.2002

31 Chugh, S., Bahal, R. K., Dhiman, R. & Singh, R. Antigen identification strategies and preclinical evaluation models for advancing tuberculosis vaccine development. *npj Vaccines* **9**, 57-57 (2024). https://doi.org/10.1038/s41541-024-00834-y

32 Leung-Theung-Long, S. *et al.* A multi-antigenic MVA vaccine increases efficacy of combination chemotherapy against Mycobacterium tuberculosis. *PloS one* **13**, e0196815-e0196815 (2018). https://doi.org/10.1371/journal.pone.0196815

33 An, Y. *et al.* Tuberculosis vaccines and therapeutic drug: challenges and future directions. *Molecular Biomedicine* **6**, 4-4 (2025). https://doi.org/10.1186/s43556-024-00243-6

34 Pagani, T. D. *et al.* Impact of Genomic Deletion RD16 on the Expression of the Mycobacterium bovis BCG Moreau VapBC47 Toxin-Antitoxin System. *Current Issues in Molecular Biology* **45**, 6538-6549 (2023). https://doi.org/10.3390/cimb45080412

35 Looney, M. M. *et al.* Conference report: WHO meeting summary on mRNA-based tuberculosis vaccine development. *Vaccine* **41**, 7060-7066 (2023). https://doi.org/10.1016/j.vaccine.2023.10.026

36 Akondy, R. S. *et al.* Origin and differentiation of human memory CD8 T cells after vaccination. *Nature* **552**, 362-367 (2017). https://doi.org/10.1038/nature24633

37 Fuertes Marraco, S. A. *et al.* Long-lasting stem cell–like memory CD8 ⁺ T cells with a naïve-like profile upon yellow fever vaccination. *Science Translational Medicine* **7** (2015). https://doi.org/10.1126/scitranslmed.aaa3700

38 Gattinoni, L., Speiser, D. E., Lichterfeld, M. & Bonini, C. T memory stem cells in health and disease. *Nature Medicine* **23**, 18-27 (2017). https://doi.org/10.1038/nm.4241

39 Hagan, T. *et al.* Transcriptional atlas of the human immune response to 13 vaccines reveals a common predictor of vaccine-induced antibody responses. *Nature Immunology* **23**, 1788-1798 (2022). https://doi.org/10.1038/s41590-022-01328-6

40 Zhao, X., Shan, Q. & Xue, H.-H. TCF1 in T cell immunity: a broadened frontier. *Nature Reviews Immunology* **22**, 147-157 (2022). https://doi.org/10.1038/s41577-021-00563-6

41 Zhou, X. *et al.* Differentiation and Persistence of Memory CD8+ T Cells Depend on T Cell Factor 1. *Immunity* **33**, 229-240 (2010). https://doi.org/10.1016/j.immuni.2010.08.002

42 Arunachalam, A. B. in *Vaccines* Vol. 12 (Multidisciplinary Digital Publishing Institute (MDPI), 2024).

43 Mettelman, R. C., Allen, E. K. & Thomas, P. G. in *Immunity* Vol. 55 749-780 (Cell Press, 2022).

44 Bartholomeus, E. *et al.* Transcriptome profiling in blood before and after hepatitis B vaccination shows significant differences in gene expression between responders and non-responders. *Vaccine* **36**, 6282-6289 (2018). https://doi.org/10.1016/j.vaccine.2018.09.001

45 Kotliarov, Y. *et al.* Broad immune activation underlies shared set point signatures for vaccine responsiveness in healthy individuals and disease activity in patients with lupus. *Nature Medicine* **26**, 618-629 (2020). https://doi.org/10.1038/s41591-020-0769-8

46 Muyanja, E. *et al.* Immune activation alters cellular and humoral responses to yellow fever 17D vaccine. *Journal of Clinical Investigation* **124**, 3147-3158 (2014). https://doi.org/10.1172/JCI75429

47 Pereira, B., Xu, X. N. & Akbar, A. N. in *Frontiers in Immunology* Vol. 11 (Frontiers Media S.A., 2020).

48 Blake, J. A. *et al.* Distal airway epithelial progenitors mediate TGF-β release to drive lung CD8+ TRM induction following mucosal BCG vaccination. *Mucosal Immunology* **18**, 973-988 (2025). https://doi.org/10.1016/j.mucimm.2025.05.007

49 Chandrashekar, A. *et al.* Vaccine protection against the SARS-CoV-2 Omicron variant in macaques. *Cell* **185**, 1549-1555.e1511 (2022). https://doi.org/10.1016/j.cell.2022.03.024

50 McMahan, K. *et al.* Mucosal boosting enhances vaccine protection against SARS-CoV-2 in macaques. *Nature* **626**, 385-391 (2024). https://doi.org/10.1038/s41586-023-06951-3

51 Vu, M. N. *et al.* Deconvolution of cargo delivery and immunogenicity following intranasal delivery of mRNA lipid nanoparticle vaccines. *Molecular Therapy Nucleic Acids* **36** (2025). https://doi.org/10.1016/j.omtn.2025.102547

52 Jennewein, M. F. *et al.* Intranasal replicon SARS-CoV-2 vaccine produces protective respiratory and systemic immunity and prevents viral transmission. *Molecular Therapy* **33**, 3286-3306 (2025). https://doi.org/10.1016/j.ymthe.2025.04.007

53 De Voss, C. J. *et al.* Novel mRNA vaccines induce potent immunogenicity and afford protection against tuberculosis. *Front Immunol* **16**, 1540359 (2025). https://doi.org/10.3389/fimmu.2025.1540359

54 Lukeman, H. *et al.* An LNP-mRNA vaccine modulates innate cell trafficking and promotes polyfunctional Th1 CD4(+) T cell responses to enhance BCG-induced protective immunity against Mycobacterium tuberculosis. *EBioMedicine* **113**, 105599 (2025). https://doi.org/10.1016/j.ebiom.2025.105599

55 Korompis, M. *et al.* Enhancing tuberculosis vaccine efficacy with a heterologous mRNA-ChAdOx1 prime-pull strategy targeting lung-resident memory T cells. *Front Immunol* **17**, 1807190 (2026). https://doi.org/10.3389/fimmu.2026.1807190

56 Kon, O. M., Edwards, M. & Endeladze, T. in *http://isrctn.com/*.

57 Tomkinson, N., Tomkinson, N. & Koch, A. in *http://isrctn.com/*.

58 Cheng, Q. *et al.* Selective organ targeting (SORT) nanoparticles for tissue-specific mRNA delivery and CRISPR–Cas gene editing. *Nature Nanotechnology* **15**, 313-320 (2020). https://doi.org/10.1038/s41565-020-0669-6

59 Dilliard, S. A. *et al.* The interplay of quaternary ammonium lipid structure and protein corona on lung-specific mRNA delivery by selective organ targeting (SORT) nanoparticles. *Journal of Controlled Release* **361**, 361-372 (2023). https://doi.org/10.1016/j.jconrel.2023.07.058

60 Parhiz, H. *et al.* PECAM-1 directed re-targeting of exogenous mRNA providing two orders of magnitude enhancement of vascular delivery and expression in lungs independent of apolipoprotein E-mediated uptake. *Journal of Controlled Release* **291**, 106-115 (2018). https://doi.org/10.1016/j.jconrel.2018.10.015

61 Qin, Z., Bouteau, A., Herbst, C. & Igyártó, B. Z. Pre-exposure to mRNA-LNP inhibits adaptive immune responses and alters innate immune fitness in an inheritable fashion. *PLoS Pathogens* **18** (2022). https://doi.org/10.1371/journal.ppat.1010830

62 Aaby, P. *et al.* Randomized trial of BCG vaccination at birth to low-birth-weight children: Beneficial nonspecific effects in the neonatal period? *Journal of Infectious Diseases* **204**, 245-252 (2011). https://doi.org/10.1093/infdis/jir240

63 Biering-Sørensen, S. *et al.* Small randomized trial among low-birth-weight children receiving bacillus Calmette-Guéerin vaccination at first health center contact. *Pediatric Infectious Disease Journal* **31**, 306-308 (2012). https://doi.org/10.1097/INF.0b013e3182458289

64 Biering-Sørensen, S. *et al.* Early BCG-Denmark and Neonatal Mortality among Infants Weighing <2500 g: A Randomized Controlled Trial. *Clinical Infectious Diseases* **65**, 1183-1190 (2017). https://doi.org/10.1093/cid/cix525

65 Adhisivam, B. *et al.* Effect of BCG Danish and oral polio vaccine on neonatal mortality in newborn babies weighing less than 2000 g in India: multicentre open label randomised controlled trial (BLOW2). *BMJ* **390** (2025). https://doi.org/10.1136/bmj-2025-084745

66 Aaby, P. & Benn, C. S. in *Proceedings of the National Academy of Sciences of the United States of America* Vol. 109 17317-17318 (2012).

67 Covián, C. *et al.* in *Frontiers in Immunology* Vol. 10 (Frontiers Media S.A., 2019).

68 Jensen, K. J. *et al.* Seasonal variation in the non-specific effects of BCG vaccination on neonatal mortality: Three randomised controlled trials in Guinea-Bissau. *BMJ Global Health* **5** (2020). https://doi.org/10.1136/bmjgh-2019-001873

69 Kramnik, I. & Beamer, G. in *Seminars in Immunopathology* Vol. 38 221-237 (Springer Verlag, 2016).

70 Broomfield, B. J. *et al.* Transient inhibition of type I interferon enhances CD8+ T cell stemness and vaccine protection. *Journal of Experimental Medicine* **222** (2025). https://doi.org/10.1084/jem.20241148

Figure Legends

Figure 1. GFP expression by lung cells following intratracheal administration of GFP-mRNA-sLNPs. **A.** Schematic representation of GFP-mRNA formulation in stealth lipid nanoparticles (sLNPs) and intratracheal (IT) administration. Mice received either PBS (control) or 10 µg GFP-mRNA-sLNPs. Lungs were harvested 24 h and 48 h following administration. GFP expression was assessed in individual pulmonary cell populations by flow cytometry. **B.** Representative concatenated flow cytometry plots showing GFP expression in neutrophils. **C.** Number of GFP^+ interstitial macrophages (IMs), dendritic cells (DCs), and neutrophils in the lungs. **D.** Heat map showing the mean fluorescence intensity (MFI) of GFP-positive cells, including IMs, DCs, neutrophils, $EpCAM^+$ epithelial cells, and alveolar macrophages (AMs). Representative gating strategies and GFP expression plots for pulmonary cell populations are shown in Supplementary Fig. 1. Data were analysed using ordinary one-way ANOVA with Dunnett's multiple-comparison test, with each group compared to the PBS control. Symbols represent individual animals and bars indicate the mean ± SEM. $P < 0.05$.

Figure 2. Pulmonary ESAT-6 mRNA boosting induces antigen-specific and memory T-cell responses following BCG priming. A. Schematic representation of the prime-and-pull vaccination strategy using BCG::RD1 priming followed by pulmonary administration of ESAT-6-mRNA-sLNPs. **B.** C57BL/6 mice were vaccinated with BCG::RD1 either subcutaneously (SC; 1×10^6 CFU) or intratracheally (IT; 1×10^5 CFU). Following SC BCG::RD1 priming, mice received pulmonary ESAT-6-mRNA-sLNP boosting according to one of four regimens: P&P-E6 (5 µg × 1), P&P-E6 (5 µg × 2), P&P-E6 (5 µg × 3), or P&P-E6 (10 µg × 1). Antigen-specific and memory T-cell responses were analysed 28 days following primary vaccination. **C.** Number of ESAT-6 $tetramer^+$ cells in bronchoalveolar lavage fluid (BALF) and lungs. **D.** Number of $CD4^+$ and $CD8^+$ memory T-cell populations, including $CD69^+CD103^-$ cells, T_{RM}-like cells, T_{CM} cells, and T_{EM} cells, in BALF and lungs. Data were analysed using the Kruskal-Wallis test with Dunn's multiple-comparison post-test. NE = 2-3 independent experiments; *n* = 4-5 mice per group. Symbols represent individual animals and bars indicate the median and interquartile range (IQR). **P*<0.05, ***P*<0.01, ****P*<0.001, *****P*< 0.0001.

Figure 3. Immunogenicity of a multivalent mRNA prime-and-pull vaccination strategy. A. Schematic representation of the four multivalent mRNA constructs encoding eight selected *Mtb*- and BCG-derived antigens formulated in sLNPs. Hybrid F1 C57BL/6 × BALB/c mice were vaccinated with BCG either SC or IT as described previously. Prime-and-pull (P&Px8) mice received a single 10 µg pulmonary administration of the multivalent mRNA-sLNP formulation 14 days following SC BCG vaccination. Immune responses were analysed 28 days following primary vaccination. **B.** Number of $CD4^+$ and $CD8^+$ T cells in BALF, lungs, and medLN. **C.** Antigen-specific IgG and IgA responses in serum and BALF, respectively, quantified as area under the curve (AUC) from serial dilution ELISA measurements using a peptide mixture containing CFP10, Ag85B, and HspX epitopes. **D.** Percentage T_{SCM} cells in the lung and medLN. **E.** Number of $CD4^+$ memory T-cell populations, including $CD69^+CD103^-$ cells, T_{RM}-like cells, T_{CM} cells, and T_{EM} cells, in BALF, lungs, and medLN. Data were analysed using the Kruskal-Wallis test with Dunn's multiple-comparison post-test. NE = 2 independent experiments; *n* = 4-5 mice per group. Symbols represent

individual animals and bars indicate the median and IQR. *P<0.05, **P<0.01, ***P<0.001, ****P< 0.0001.

Figure 4. Prime-and-pull vaccination reduces bacterial burden following *Mtb* challenge and induces a lower inflammatory profile than intratracheal BCG vaccination. In **A-C**, C57BL/6 mice were vaccinated with BCG::RD1 either SC or IT. Prime-and-pull mice received a single 10 µg pulmonary administration of ESAT-6-mRNA-sLNPs 14 days following SC BCG::RD1 vaccination. In **D-G**, hybrid F1 C57BL/6 × BALB/c mice were vaccinated with BCG either SC or IT. Prime-and-pull (P&Px8) mice received a single 10 µg pulmonary administration of the multivalent mRNA-sLNP formulation 14 days following SC BCG vaccination. Sixty days after vaccination, mice were challenged by very low-dose aerosol infection with *Mtb* H37Rv. Bacterial burden and lung pathology were assessed 45 days post-infection. **ESAT-6 model: A.** Lung bacterial burden. **B.** Percentage of lung tissue area exhibiting dense inflammatory cellular infiltration. **C.** Representative H&E-stained lung sections. **Multivalent mRNA formulation: D.** Lung bacterial burden. **E.** Percentage of lung tissue area exhibiting dense inflammatory cellular infiltration. **F.** Representative H&E-stained lung sections. **G.** Serum cytokine and chemokine concentrations displayed as a heatmap of log_2-transformed values. Bacterial burden data were log_{10}-transformed and analysed using one-way ANOVA with Tukey's multiple-comparison post-test. Pathology data were analysed using the Kruskal-Wallis test with Dunn's multiple-comparison post-test. NE = 2 independent experiments; n = 5 mice per group. Symbols represent individual animals. For bacterial burden analyses, bars indicate the mean ± SEM of log_{10}-transformed data. For pathology analyses, bars indicate the median and IQR. *P<0.05, **P<0.01, ***P<0.001, ****P< 0.0001.

Figure 5. Prime-and-pull vaccination induces local immune responses while limiting pulmonary inflammation. A-C. Data from the ESAT-6 model. **D-F.** Data from the multivalent mRNA formulation. Mice were vaccinated as described in Fig. 2 and Fig. 3, respectively. Cytokine producing T cell and pulmonary pathology were assessed 28 days following vaccination. **ESAT-6 model: A.** Number of lung ESAT-6 tetramer$^+$ and total CD8$^+$ T cells producing IFN-γ, TNF-α, and IL-2. **B.** Percentage of lung tissue area exhibiting dense inflammatory cellular infiltration 4 weeks following vaccination. **C.** Integrated heatmap summarizing inflammatory, immunological, and protection-associated parameters. **Multivalent mRNA formulation: D.** Number of lung Ag85B tetramer$^+$ and total CD8$^+$ T cells producing IFN-γ, TNF-α, and IL-2. **E.** Percentage of lung tissue area exhibiting dense inflammatory cellular infiltration 4 weeks following vaccination. **F.** Integrated heatmap summarizing inflammatory, immunological, and protection-associated parameters. Data were analysed using the Kruskal-Wallis test with Dunn's multiple-comparison post-test. NE = 2-3 independent experiments; n = 4-5 mice per group. Symbols represent individual animals and bars indicate the median and IQR. *P<0.05, **P<0.01, ***P<0.001, ****P< 0.0001.

Supplementary Files

This is a list of supplementary files associated with this preprint. Click to download.

- CombinedSuppFigs15.pdf